



Quantitative magnetic resonance imaging for determining bone marrow fat fraction at 1.5 T and 3.0 T: a technique to noninvasively assess cellularity and potential malignancy of the bone marrow

Jonathan D. Samet¹ · Jie Deng² · Kristian Schafernak³ · Nicoleta C. Arva⁴ · Xiaoqi Lin⁵ · Joseph Peevey⁶ · Laura M. Fayad⁷

Received: 4 May 2020 / Revised: 3 July 2020 / Accepted: 10 August 2020 / Published online: 5 September 2020
© Springer-Verlag GmbH Germany, part of Springer Nature 2020

Abstract

Background Pediatric bone marrow assessment by MRI is challenging and primarily experiential and qualitative, with a paucity of clinically useful quantitative imaging techniques.

Objective MRI fat fraction (MRI-FF) is a technique used to quantify the degree of fat in other organ systems. The purpose of this study was to assess whether MRI-FF accurately measures bone marrow composition.

Materials and methods This two-part study included a validation phase, followed by an application phase. For the validation phase, the MRI-FF of piglet bones (6 long bones, 8 axial bones) was performed at 1.5 tesla (T) and 3.0 T, and correlated to the histological fat fraction (H-FF). We used Bland–Altman plots to compare MRI-FF at 1.5 tesla T and 3.0 T. For the application phase, five children with malignant marrow disease were recruited along with seven age- and gender-matched control subjects. The MRI-FF in the children was correlated to the H-FF. Boxplots were used to compare the MRI-FF of patients and control subjects.

Results For the validation animal study, the MRI-FF of piglet bones at both 1.5 T and 3.0 T demonstrated moderate positive correlation to H-FF ($r=0.41$ and 0.42 , respectively). MRI-FF at 1.5 T and 3.0 T were in good agreement, on average 7.7% apart. For the application phase, we included 5 children (4 with leukemia, 1 rhabdomyosarcoma) with median age 7 years, range (3–10 years). All children had MRI-FF and H-FF below 10%. The MRI-FF in patients (3.8 ± 1.2) was significantly lower than that of control subjects ($46.1\pm 12.3\%$) ($P<0.01$).

Conclusion MRI-FF is a valid technique to assess bone marrow fat fraction at both 1.5 T and 3.0 T. The MRI-FF in children with malignant marrow processes is significantly lower than in control subjects with normal marrow.

Keywords Bone marrow · Cellularity · Children · Diffuse marrow process · Fat fraction · Magnetic resonance imaging

Introduction

Bone marrow assessment is routinely performed with MRI but is a difficult task because of the highly variable appearance of

normal marrow [1]. In particular, pediatric marrow imaging is challenging because the proportion of red marrow relative to fatty marrow changes drastically with age [2, 3].

✉ Jonathan D. Samet
jsamet@luriechildrens.org

¹ Ann & Robert H. Lurie Children’s Hospital of Chicago, Northwestern University Feinberg School of Medicine, 225 E. Chicago Ave., Chicago, IL 60611, USA

² Department of Diagnostic Radiology and Nuclear Medicine, Rush University Medical Center, Chicago, IL, USA

³ Department of Pathology and Laboratory Medicine, Phoenix Children’s Hospital, Phoenix, AZ, USA

⁴ Pathology Department, Ann & Robert H. Lurie Children’s Hospital of Chicago, Northwestern University Feinberg School of Medicine, Chicago, IL, USA

⁵ Department of Pathology, Northwestern Memorial Hospital, Northwestern University, Chicago, IL, USA

⁶ Department of Pathology, OSF Healthcare, St. Anthony Hospital, Rockford, IL, USA

⁷ Russell H. Morgan Department of Radiology and Radiological Science, Johns Hopkins School of Medicine, Baltimore, MD, USA

Bone marrow evaluation is primarily qualitative, with T1-weighted and fluid-sensitive sequences used as the mainstay methods for marrow assessment [1, 4]. A comparison of marrow signal intensity to adjacent muscle is used to determine whether the marrow is hypercellular, hypocellular or normocellular [1]; the process is subjective, non-quantitative, and relies heavily on the experience of the radiologist. Not surprisingly, the interpretation can be flawed with errors of omission or misinterpretation, or a nonspecific differential diagnosis [1].

The bone marrow is composed of red (hematopoietic) marrow and yellow (fat) marrow, and the marrow fat fraction is inversely related to the degree of bone marrow cellularity [5]. Several methods have been used for determining fat fraction in the marrow including MR spectroscopy [6], a cumbersome technique that is not routinely incorporated clinically, and the two-point Dixon method. With the latter technique, a drop in signal on opposed-phase compared with in-phase imaging, of 20% at 1.5 tesla (T) or 15% at 3.0 T [7], rules out a marrow-replacing process. However, the Dixon method, although clinically useful, is only sensitive for detecting malignant bone marrow processes when a threshold degree of disease infiltration has occurred [2]. Without the threshold-required proportion of infiltrative cells, false-negative results in bone marrow interpretation occur and can lead to a delay in the diagnosis of a malignancy. Conversely, misinterpreting dense red marrow as disease can lead to unnecessary marrow biopsies. Therefore, a more accurate quantitative assessment of the marrow fat fraction would be a critically important adjunctive technique to bone marrow evaluation.

MRI fat fraction (MRI-FF) is a technique to provide a non-invasive method for the quantification of fat within the liver [8]. Our hypothesis was that the MRI-FF is a feasible technique for quantifying marrow composition and that it accurately correlates with the histological makeup of the marrow. Therefore, the purpose of this investigation was to validate the multipoint Dixon MRI-FF technique for assessing bone marrow composition using an animal model, at both 1.5 T and 3.0 T, and to apply the sequence to subjects with infiltrative malignant marrow processes.

Materials and methods

Study design

This study was approved by our institutional review board and complied with the Health Insurance Portability and Accountability Act. The study was performed in two phases, a validation phase of the MRI-FF technique in bone marrow, and an application phase of the technique in children with suspected malignant marrow processes.

For the validation phase, we assessed the FF technique in piglet bones (all from one piglet) at 1.5 T and 3.0 T because both field strengths are routinely used in clinical practice. We investigated multiple bone sites (long bones and axial skeleton) to robustly assess the accuracy of MRI-FF compared to a histological analysis. Following MRI, the bones were sliced in an anatomy lab (by musculoskeletal-trained radiologist with 6 years of post-fellowship experience, J.D.S.) and carefully labeled to correlate precisely with the regions sampled on MRI. One pathologist (K.S., a hematopathologist with 16 years of experience) reported the histological fat fraction (H-FF) for each region, without knowledge of the bone site and MRI-FF.

For the application phase, we recruited children with MRI-suspected malignant marrow processes and performed MRI-FF. All children had true malignant marrow replacement (confirmed by bone marrow biopsy). Two pathologists (N.C.A., with 13 years of experience, and K.S.), blinded to clinical factors, interpreted pathology samples.

Validation phase

Animal specimens

Piglet bones were procured from an animal lab, where bones were discarded following unrelated solid organ research focused on cardiovascular conditions. There were no known marrow conditions. The soft tissues were removed and whole intact bones were obtained and refrigerated. These bones included cervical and lumbar spine vertebrae, sacrum, ilium, bilateral humeri, bilateral femora and bilateral tibiae.

Magnetic resonance imaging acquisition

Each bone was scanned on two scanners, 1.5 T (Aera; Siemens Healthcare, Erlangen, Germany) and 3.0 T (Skyra; Siemens). We obtained a T1-weighted non-fat-suppressed sequence for each body part for anatomical localization. Multipoint Dixon volumetric interpolated breath-hold examination (VIBE) sequence was then performed using the following parameters: field of view (FOV)= $200 \times 100 \text{ mm}^2$; repetition time (TR)=120 ms; echo time (TE)=2.3–13.8 ms with $\Delta\text{TE}=2.3 \text{ ms}$ on 1.5 T, and TE=1.2–6.9 ms with $\Delta\text{TE}=1.2 \text{ ms}$ on 3.0 T, with each TE corresponding to consecutive in-phase and out-of-phase TE; matrix = 192×96 ; slice thickness = 4 mm; number of slices = 3; flip angle 10° [9, 10]. The scanner console displayed inline images of water signal and fat signal, and parametric maps of fat percentage and $R2^*$, allowing for region-of-interest (ROI) analysis. ROIs were hand-drawn by one observer (J.D.S.) on the fat percentage map for each specific bone (Fig. 1). In a long bone, because the epiphyses, diaphyses and metaphyses are known to have different proportions of yellow and red marrow [1],



Fig. 1 Coronal MRI of a piglet bone scanned on a 1.5-T scanner. **a** T1-weighted image for anatomical localization. **b** Fat-only Dixon image with regions of interest placed over the proximal and distal metaphyses

additional ROIs were placed at these locations. The ROI was drawn to capture the entire region, such as the entire metaphysis (Fig. 1). Three ROIs at consecutive slices were drawn for each area and the average fat fraction was recorded. For example, in a given long bone, the epiphyses ($\times 2$), metaphyses ($\times 2$) and diaphysis were sampled, producing 5 data points for each long bone. A cervical vertebra, lumbar vertebra, sacral vertebra and bilateral posterior iliac crests were also sampled. There were a total of 38 data points from a total of 14 bone sections. This method was duplicated for the 3-T scan using the same piglet bones. The techniques for 1.5 T and 3.0 T were identical.

Magnetic resonance imaging fat fraction

Fat fraction maps were generated based on the Dixon method ($FF = \text{fat}/\text{water} + \text{fat} = [\text{in-phase} - \text{out-of-phase}]/2 \times \text{in-phase}$) [8]. The mean and standard deviation of FF values within each ROI of each area of bone marrow were recorded directly from the FF maps. The number obtained from the ROI was divided by 10 to give the fat fraction percentage, which is based on the Siemens post-processing algorithm. The MRI-FF sequence is short, approximately 2.5 min.

Histological fat fraction

The piglet bones were sectioned into small pieces, with the creation of a thin slice that corresponded to the locations of ROIs used for the MRI. Bone samples were then decalcified and hematoxylin and eosin stain slides produced for each site;

100x magnified slides were produced. The slides were interpreted by one pathologist (K.S.) who was blinded to the bone site and MRI-FF. An H-FF was recorded for each bone site and was determined as follows: as is standard practice in hematopathology [11], bone marrow cellularity was visually estimated and expressed as the percentage of the marrow cavity occupied by hematopoietic cells over the total of both hematopoietic cells and adipocytes. The FF was determined by subtracting the percentage cellularity from 100%.

Investigation of human subjects

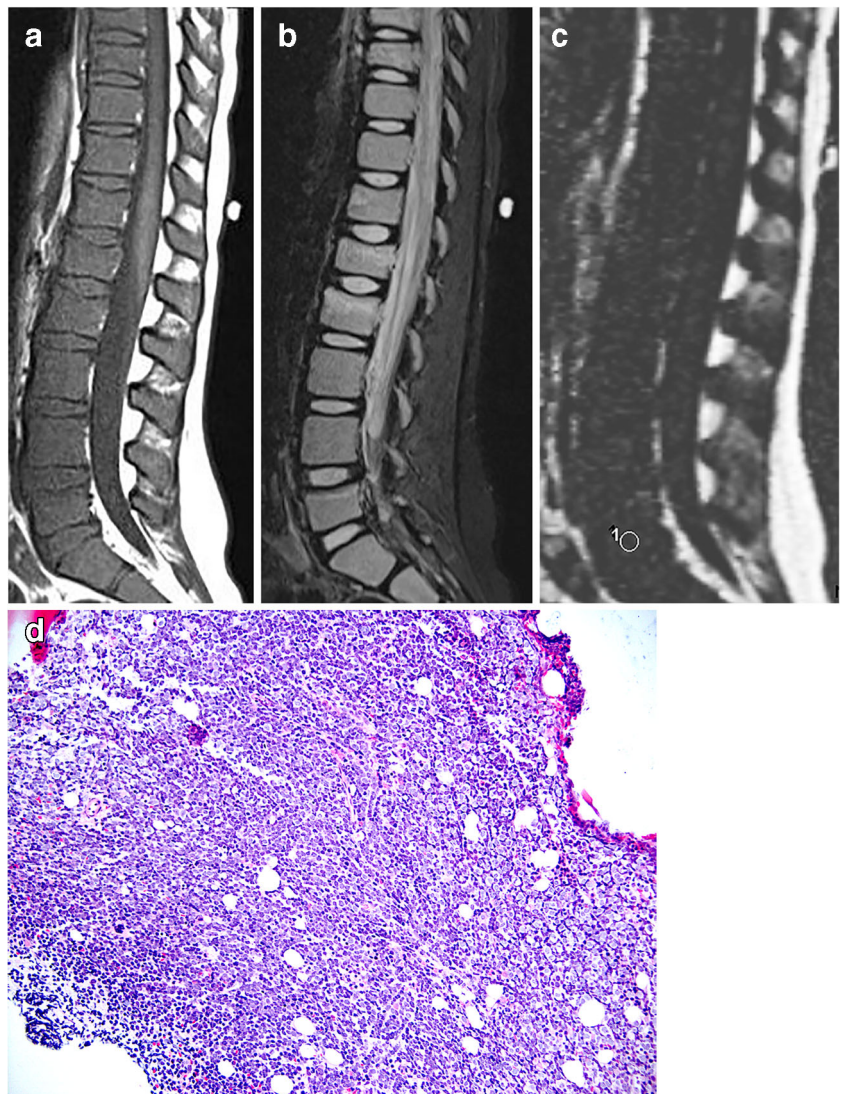
Inclusion criteria for the clinical cases were children with suspected malignant marrow replacement on conventional MRI sequences. If the interpreting radiologist thought there was a possible malignant marrow process on the routine MR sequences, the fat-fraction sequence was added to the scan. Therefore, each clinical case was scanned during a single MRI examination. Five children were recruited by this method between September 2014 and August 2018, all presenting to the emergency department. Five children had bone pain; four had no known diagnosis of malignancy, and one was suspected of having a rhabdomyosarcoma relapse. MRI and bone marrow biopsy of all five children were performed within 1–4 days (mean 2.5 days) of each other.

MRI acquisition included two-plane conventional T1-weighted spin-echo ($TR/TE=624/9.7$ ms), fat-suppressed T2-weighted ($TR/TE=6,190/74$ ms) and short tau inversion recovery (STIR; $TR/TE=5,810/46$ ms) sequences, and the multipoint Dixon technique as used for the animal specimens. All five children were scanned on 1.5-T scanners. The pelvis was examined in four cases and the spine in one. Regions of interest for the pelvis were placed along the posterior iliac crest, so as to be similar to the location for bone marrow biopsy. In the case of the spine MRI, the ROI was placed in the mid L5 vertebral body (Fig. 2). ROIs were placed using a clinical picture archiving and communication (PACS) station.

A biopsy of the bone marrow was performed by the oncologist, of the posterior iliac crest, as part of standard clinical care. An 11- or 13-gauge needle was used and at least one core was obtained in each case. The two pathologists determined the bone marrow FF and recorded an average of their measurements. An H-FF was determined using the same method as that used for analysis of the pig bone marrow. In one of the human cases, only aspirate smears were available; nevertheless, bone marrow cellularity (and its inverse, the fat fraction) was assessed by examination of several bone marrow particles in the stained smears.

Inclusion criteria for the controls were age and anatomically matched children with no known hematologic conditions who were undergoing MRI of the pelvis and spine for other reasons (Table 1). Five control patients were scanned at 1.5 T and two at 3.0 T.

Fig. 2 MR imaging in a 7-year-old girl with back pain and elevated inflammatory markers. **a–c** Sagittal T1 (**a**), sagittal short tau inversion recovery (STIR; **b**) and sagittal fat-only Dixon (**c**) MR images of the lumbar spine. Routine sequences show diffuse T1 hypointensity and STIR hyperintensity of the bone marrow, initially thought to be related to red marrow conversion. **d** Bone marrow biopsy core with hematoxylin-eosin stain (200x magnification) shows hypercellular bone marrow infiltrated by leukemic cells with minimal fat, 4.5%



Statistical analysis

First, for the validation phase, the MRI-FF in the pig bone specimens obtained at 1.5 T and 3.0 T were graphed and compared to the H-FF for each bone site. We used correlation testing to assess the agreement between MRI-FF and H-FF at each field strength, in each of the specimens. Second, for the application phase in the human subjects investigation, the MRI-FF was similarly compared to the H-FF using correlation testing.

For human studies, we used descriptive statistics to describe patient characteristics, and we compared correlations and means using non-parametric statistics because of the small sample size. Boxplots were generated to compare the patients with marrow replacement and age-matched controls. For animal studies, because of the larger sample size, we used parametric statistics.

We used a Bland–Altman plot to compare MRI-FF at 1.5 T and 3.0 T. Pearson correlations were planned to compare H-FF to MRI-FF. We used SPSS version 23 (IBM, Armonk, NY).

Results

Validation phase: animal study

In 14 piglet bones, we obtained 38 MRI-FF values at both 1.5 T and 3.0 T. Figure 1 is a representative image, displaying the piglet femur at 1.5 T. This figure demonstrates the methodology of selecting the region of interest — in this example the proximal and distal metaphysis — for MRI-FF calculation. The bones analyzed included bilateral tibiae ($n=2$), bilateral femora ($n=2$), bilateral humeri

Table 1 Demographic data for patients with malignancy and control subjects

Demographics and data	Patients (<i>n</i> =5)	Controls (<i>n</i> =7) ^a	<i>P</i> -value ^b
Age, mean in years (range)	7.3 (3–10)	7.5 (1–13)	0.95 ^c
Male, % (<i>n</i>)	40% (2/5)	71% (5/7)	0.56 ^d
Location, % (<i>n</i>)			
Spine	20% (1/5)	14% (1/7)	0.79
Ilium	80% (4/5)	86% (6/7)	
Listed indication for MRI, % (<i>n</i>)			
Bone pain	100% (5/5)	28% (2/7)	0.16
Possible vascular anomaly		28% (2/7)	
Possible avascular necrosis		28% (2/7)	
Possible genitourinary anomaly		14% (1/7)	
Diagnosis of malignancy known at time of MRI	20% (1/5)	n/a	
MRI findings, % (<i>n</i>)			
Diffuse T2-hyperintense bone marrow signal	100% (5/5)	0% (0/7)	
Diffuse T1-hypointense bone marrow signal	100% (5/5)	0% (0/7)	
T1 signal hypointense to skeletal muscle	100% (5/5)	0% (0/7)	
MRI fat fraction, mean % (SD)	3.8% (1.2)	46.1% (12.3)	<0.01
Bone marrow biopsy performed, % (<i>n</i>)	100% (5/5)	0% (0/7)	
Time between biopsy/MRI, days (mean±SD)	2.5±1.1	n/a	
Pathology finding, % (<i>n</i>)			
Leukemia	80% (4/5)	n/a	
Rhabdomyosarcoma	20% (1/5)	n/a	

n number/total, *n/a* not applicable, *SD* standard deviation

^a Controls were matched by age and anatomical location. All patients with malignancy had diffuse marrow replacement on conventional MRI sequences. MRI fat fraction in all patients with malignancy was below 10% and significantly less than controls

^b *P*<0.05 is significant

^c *t*-test

^d Chi-square test

(*n*=2), cervical spine vertebrae (*n*=3), lumbar/sacral spine vertebrae (*n*=3) and bilateral iliac bones (*n*=2). Within each long bone, as expected, there were different degrees of cellularity in the epiphyses, metaphyses and diaphysis (MRI-FF 35.9±7.2%, 18.5±3.2%, 47.8±11.5%, respectively). With regard to cellularity in different body regions, we found the pelvis, spine and extremity of the piglet bone to have mean MRI-FF 15.5±7.2%, 24.8±3.1%, 31.3±13.4%, respectively.

Moderate correlation of the measurements was obtained at 1.5 T and 3.0 T when comparing MRI-FF to H-FF (*r*=0.41 and *r*=0.42, respectively), as shown in Fig. 3. The MRI-FFs at 3.0 T were on average 7.7% lower than at 1.5 T, which is visualized using a Bland–Altman plot (Fig. 3). In addition, Bland–Altman plots show the relationship between 1.5 T to H-FF and 3.0 T to H-FF (Fig. 3).

Applications phase: human subjects study

We recruited five children with malignant marrow replacement processes (median age 7 years; range 3–10 years; 2 boys, 3 girls).

A convenience sample of seven controls with no previous hematologic condition was also recruited (mean age 7.5 years; range 1–13 years; 4 boys, 3 girls). Histological diagnoses in the children with malignancy included leukemia (*n*=4) and rhabdomyosarcoma (*n*=1). We analyzed MRI-FFs from the pelvis (*n*=4) and spine (*n*=1). Demographics of the patient population, MRI-FFs and signal characteristics on T1- and T2-weighted images are summarized in Table 1.

Regarding the bone marrow biopsies, inter-pathologist scoring for H-FF was within 2.2% between scorers. In children with malignant marrow processes, the MRI-FFs and H-FFs were all below 10% (H-FF/MRI-FF=4.5/3.1, 0.5/4.1, 7.5/5.7, 1.3/2.5, 2.6/2.5), although they were not significantly correlated in this small data set *r*_s=0.36, *P*=0.55. Although no biopsy was obtained in controls, the MRI-FFs were all above 20% (Fig. 4). The average MRI-FF of the controls was 46.1%, with a standard deviation of 12.3%. Figure 5 demonstrates the significant difference observed in the MRI-FF between the malignant marrow and the control marrow (*P*<0.01). Examples of the MRI findings closely resembling the pathological findings are given in Figs. 2, 6, 7 and 8.

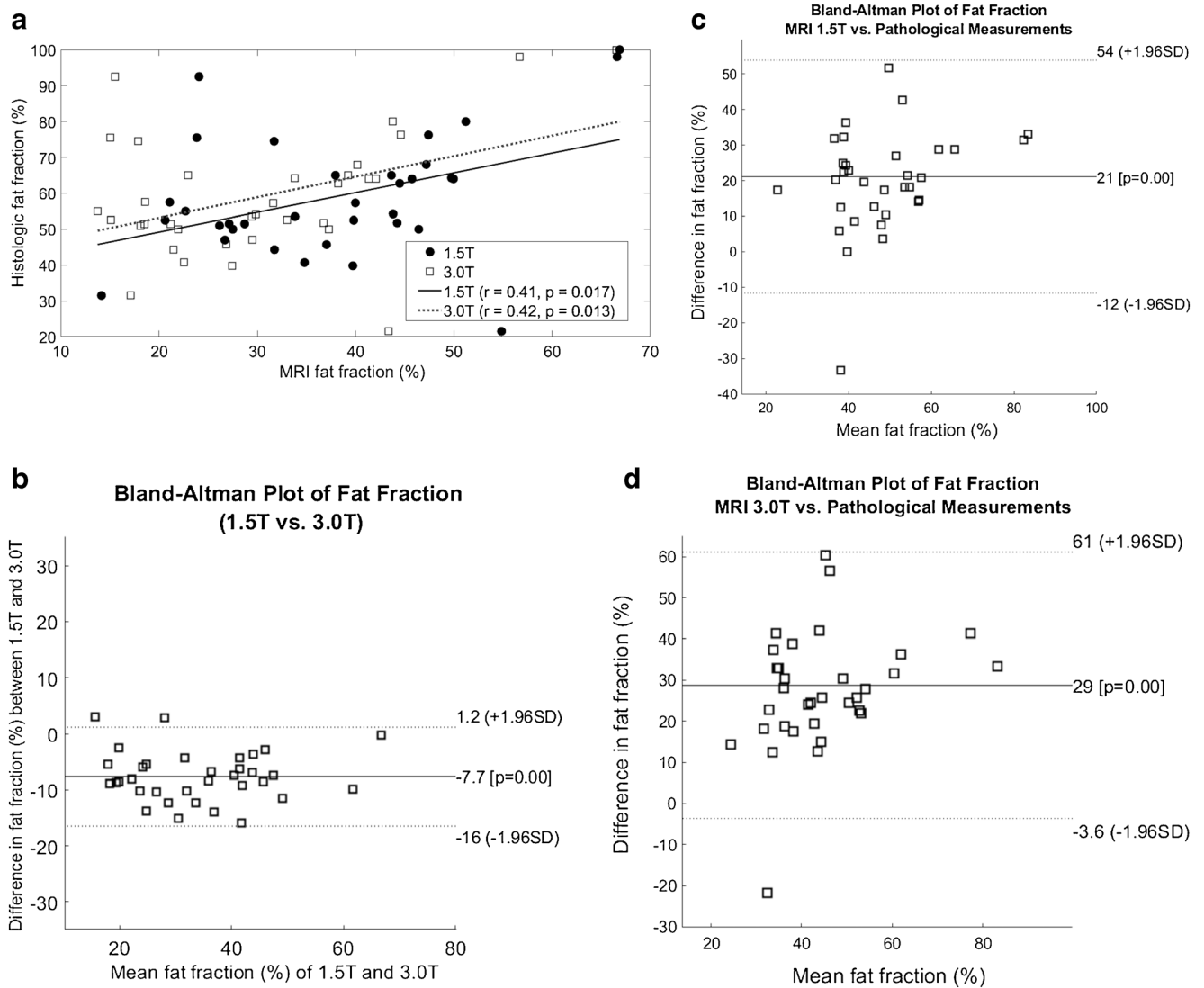


Fig. 3 Correlation plot between fat fraction (FF) measured by MRI and FF determined by histological analysis. **a** Both 1.5-T and 3.0-T MRI fat percentage correlated moderately well with histological results. **b** MRI-FF measured at 1.5 T and 3.0 T are compared using a Bland–Altman plot. Mean is the averaged $FF_{1.5T}$ and $FF_{3.0T}$, and Δ is the difference between

$FF_{3.0T}$ and $FF_{1.5T}$. FF measured at 3.0 T is on average 7.7% lower than that on 1.5 T (standard deviation [SD] of mean values in %). **c** Bland–Altman plot compares 1.5 T to histological fat fraction (H-FF). **d** Bland–Altman plot compares 3.0 T to H-FF

Discussion

The MRI interpretation of pediatric bone marrow is a challenging task because of the highly variable degree of red marrow in children and the resultant difficulty of differentiating marrow replacement processes such as leukemia from red marrow. In this investigation, we showed that the measurement of the MRI-FF of marrow is feasible and valid, correlating moderately to the H-FF at both 1.5 T and 3.0 T in an animal model. Furthermore, in human subjects, the MRI-FF was found to be significantly different in children with malignancy compared to those with normal bone marrow, with the FF in all children with malignancy less than 10%.

Although the FF in bone marrow normally increases as childhood progresses (because of conversion to fatty marrow), a normal value for a 2-year-old is 20% and for young adults is up to 30–40% [11, 12]. Therefore, with malignancy found to have a FF less than 10% in our sample, the FF technique described in our investigation can be used as a simple low-cost method to confirm suspected malignancy and serve as a helpful adjunct for the radiologist to determine the likelihood of malignant marrow.

In our study, we used a multi-echo Dixon volumetric interpolated breath-hold examination (VIBE) technique, which enables comprehensive fat quantification through the mapping of fat and water percentages and $R2^*$.

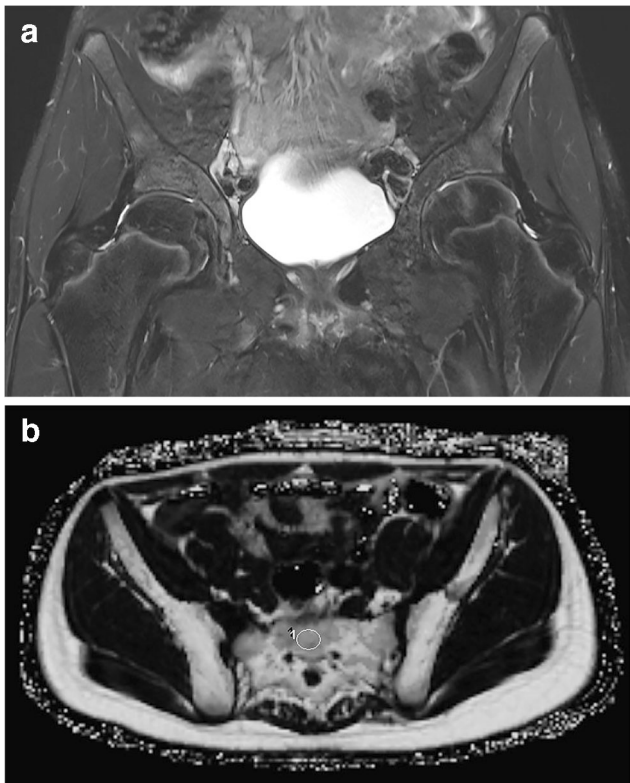


Fig. 4 Imaging in a control 12-year-old girl with no known hematologic condition. **a, b** Coronal short tau inversion recovery (STIR; **a**) and fat-only Dixon axial MR image with region of interest placed over the sacrum (**b**) demonstrate a fat percentage of 46%, or 54% cellularity

Accurate tissue fat quantification is confounded by T2* signal decay, field inhomogeneities, the spectral

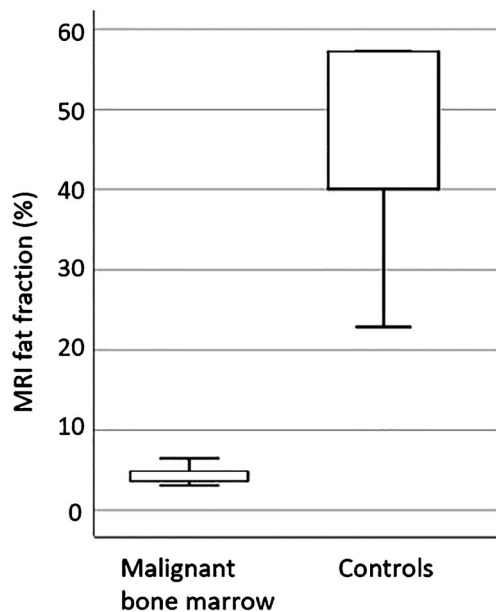


Fig. 5 Boxplot shows malignant marrow cases compared to controls ($P=0.004$). Children with malignant bone marrow had very low fat fraction, all below 10%, because of the high cellularity, whereas control subjects had a much higher fat fraction

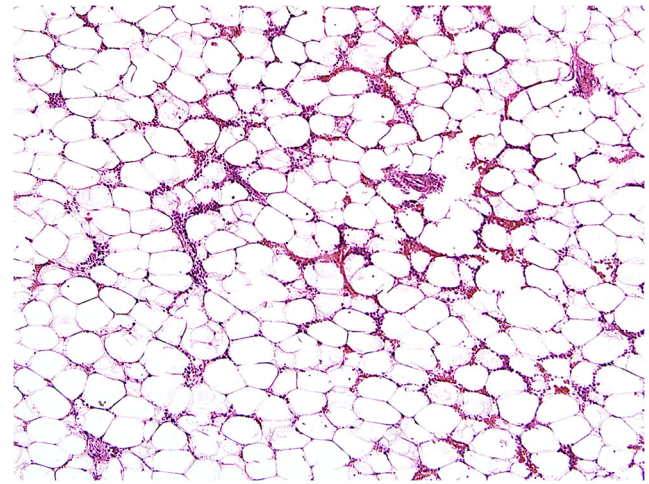


Fig. 6 Bone marrow slide of a piglet tibial diaphysis. Hematoxylin-eosin stained section, 200x magnification. The marrow is extremely fatty, with a fat fraction of 98%

complexity of the fat molecules, and T1 effects. The multi-echo Dixon VIBE sequence addresses these challenges by compensating for all of these confounding effects by using a low flip angle to reduce T1 effects, accounting for the spectral complexity of the fat in the signal model, and utilizing nonlinear fitting for simultaneous estimation of fat and R2* ($1/T2^*$) [8]. This noninvasive technique has proved very useful in the assessment of fatty liver disease [8, 10]. Although this technique has been applied to evaluate bone marrow FF, specifically focal bone lesions [13], osteoporosis [14] and development [15], to our knowledge, this is the first application of this technique to study marrow replacement in pediatric malignancy.

In addition to our investigation, other studies have examined MRI-FF techniques to assess cellularity and fat fraction by MRI [16, 17] and shown that MRI-FF correlates with H-FF. However, these studies were both performed on 3.0-T systems only. In our study, we validated the technique at 1.5 T and 3.0 T because both scanner types remain in clinical use. We showed that values derived at 1.5 T and 3.0 T are similar, and therefore in our opinion, the technique can be used interchangeably at 1.5 T or 3.0 T. To our knowledge, this pilot investigation is the first to show that MRI-FF technique is valid at 1.5 T and 3.0 T and that values derived by MRI are in good agreement with those derived histologically.

The use of MRI-FF could have important implications to the clinical workflow in children with malignant marrow disease: bone marrow biopsy, an invasive procedure, is the gold standard for diagnosing leukemia. If a noninvasive method with MRI is available for diagnosing leukemia, the next step in the workup of a child with suspected leukemia could include fluorescence in situ hybridization (FISH) and karyotyping of the peripheral blood, to confirm a high



Fig. 7 Imaging in a 10-year-old boy with metastatic rhabdomyosarcoma. **a–c** Axial T1 (**a**), axial short tau inversion recovery (STIR; **b**) and axial fat-only Dixon (**c**) MR images of the pelvis. Routine sequences show diffuse T1 hypointensity and STIR hyperintensity of the bone marrow. There is also abnormal soft-tissue signal surrounding the left iliac wing. The MRI fat fraction (FF) shows FF of 5%, or 95% cellularity, compatible with the marrow replacement process

peripheral blood blast cell burden. In this way, bone marrow biopsy could theoretically be averted [18]. Furthermore, if a child is very sick, oncologists might elect to begin therapy immediately, without obtaining bone marrow biopsy results, another reason to pursue MRI-FF as an alternative method.

Our study has limitations, including a small number of patients. At our institution, there are approximately 30–50 new cases of acute leukemia each year. The vast majority do not undergo an MRI. Typically, if there is suspicion of leukemia, a peripheral blood sample and bone marrow biopsy are performed. MRI is used in the case of an unknown diagnosis when other diagnoses are still being considered. Therefore it was difficult to capture a large

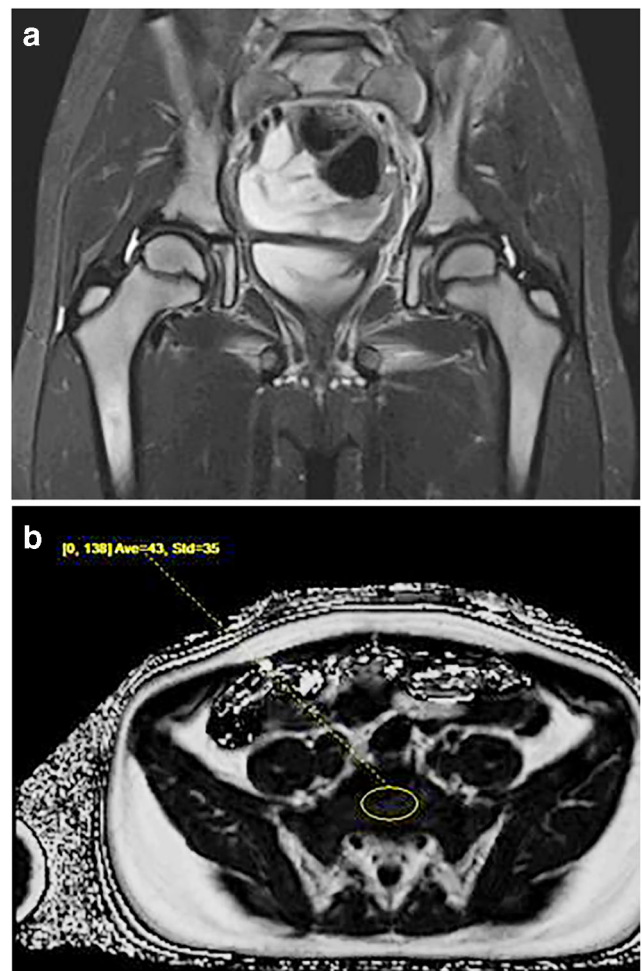


Fig. 8 Imaging in a 5-year-old girl with hip pain. **a** Coronal short tau inversion recovery (STIR) MR image shows diffuse hyperintense bone marrow signal. **b** Fat-only Dixon axial image with region of interest placed over the sacrum demonstrates fat fraction of 4%, or cellularity of 96%. Leukemia was confirmed with bone marrow biopsy

sample for inclusion in this study. Second, although the control subjects had fat fractions statistically different from those in children with malignancy, more studies are needed to determine the true range of bone marrow fat fraction for each age group. There are also known hematologic conditions with more hypercellular marrow that could have low fat fraction and produce a false-positive result of malignancy, such as sickle cell disease, thalassemia and Gaucher disease.

Conclusion

Quantitative MRI with fat-fraction analysis is a feasible technique that showed promising results for the diagnosis of hypercellular marrow in our pilot study. It is a fast non-contrast technique that can be used at 1.5 T and 3.0 T. By

quantifying bone marrow fat fraction, this technique could be used to help the radiologist suggest a malignant marrow replacement process and aid in the workup of a child with suspected leukemia.

Compliance with ethical standards

Conflicts of interest None

References

- Chan BY, Gill KG, Rebsamen SL, Nguyen JC (2016) MR imaging of pediatric bone marrow. *Radiographics* 36:1911–1930
- Shiga NT, Del Grande F, Lardo O, Fayad LM (2013) Imaging of primary bone tumors: determination of tumor extent by non-contrast sequences. *Pediatr Radiol* 43:1017–1023
- Bracken J, Nandurkar D, Radhakrishnan K, Ditchfield M (2013) Normal paediatric bone marrow: magnetic resonance imaging appearances from birth to 5 years. *J Med Imaging Radiat Oncol* 57:283–291
- Burdiles A, Babyn PS (2009) Pediatric bone marrow MR imaging. *Magn Reson Imaging Clin N Am* 17:391–409
- Matcuk GR Jr, Siddiqi I, Cen S et al (2016) Bone marrow cellularity MRI calculation and correlation with bone marrow biopsy. *Clin Imaging* 40:392–397
- Karampinos DC, Ruschke S, Dieckmeyer M et al (2018) Quantitative MRI and spectroscopy of bone marrow. *J Magn Reson Imaging* 47:332–353
- Kumar NM, Ahlawat S, Fayad LM (2018) Chemical shift imaging with in-phase and opposed-phase sequences at 3 T: what is the optimal threshold, measurement method, and diagnostic accuracy for characterizing marrow signal abnormalities? *Skelet Radiol* 47:1661–1671
- Deng J, Fishbein MH, Rigsby CK et al (2014) Quantitative MRI for hepatic fat fraction and T2* measurement in pediatric patients with non-alcoholic fatty liver disease. *Pediatr Radiol* 44:1379–1387
- Bydder M, Yokoo T, Hamilton G et al (2008) Relaxation effects in the quantification of fat using gradient echo imaging. *Magn Reson Imaging* 26:347–359
- Yokoo T, Bydder M, Hamilton G et al (2009) Nonalcoholic fatty liver disease: diagnostic and fat-grading accuracy of low-flip-angle multiecho gradient-recalled-echo MR imaging at 1.5 T. *Radiology* 251:67–76
- Friebert SE, Shepardson LB, Shurin SB et al (1998) Pediatric bone marrow cellularity: are we expecting too much? *J Pediatr Hematol Oncol* 20:439–443
- Thiele J, Kvasnicka HM, Facchetti F et al (2005) European consensus on grading bone marrow fibrosis and assessment of cellularity. *Haematologica* 90:1128–1132
- Yoo HJ, Hong SH, Kim DH et al (2017) Measurement of fat content in vertebral marrow using a modified Dixon sequence to differentiate benign from malignant processes. *J Magn Reson Imaging* 45:1534–1544
- Kuhn JP, Hernando D, Meffert PJ et al (2013) Proton-density fat fraction and simultaneous R2* estimation as an MRI tool for assessment of osteoporosis. *Eur Radiol* 23:3432–3439
- Zhang C, Slade JM, Miller F, Modlesky CM (2020) Quantifying bone marrow fat using standard T1-weighted magnetic resonance images in children with typical development and in children with cerebral palsy. *Sci Rep* 10:1–8
- Gee CS, Nguyen JT, Marquez CJ et al (2015) Validation of bone marrow fat quantification in the presence of trabecular bone using MRI. *J Magn Reson Imaging* 42:539–544
- Pichardo JC, Milner RJ, Bolch WE (2011) MRI measurement of bone marrow cellularity for radiation dosimetry. *J Nucl Med* 52:1482–1489
- Percival ME, Lai C, Estey E, Hourigan CS (2017) Bone marrow evaluation for diagnosis and monitoring of acute myeloid leukemia. *Blood Rev* 31:185–192

Publisher's note Springer Nature remains neutral with regard to jurisdictional claims in published maps and institutional affiliations.